Reply to Referee Comments

(C and R denote comment and reply, respectively)

We would like to express our sincere gratitude to you for your careful reading of our manuscript and for providing insightful and constructive comments. We have carefully considered all the comments and revised the manuscript accordingly. Below, we provide a detailed response to each comment raised by the referee.

Referee #1:

General comments:

C1: This manuscript mainly analyzes seismic signals generated by three debris flows and infrared imagery, with a focus on one event, in two catchments in Wenchuan, China. The study provides valuable seismic data that enrich the existing database of debris flow signals. The authors employ basic signal processing techniques, including short-time Fourier transform (STFT), power spectral density (PSD), and cross-correlation, to analyze these data. However, the novelty of the manuscript is questionable, as it offers limited new insights compared to previous studies, appearing more like a case study.

R1: Thank you very much for your valuable comments. Based on your recommendations, we have shifted the focus of our study from monitoring and early warning to analyzing the seismic signal characteristics of debris flows and reconstructing their movement patterns. In this study, we used methods such as short-time Fourier transform (STFT), power spectral density analysis (PSD), and cross-correlation analysis to perform an in-depth analysis of the seismic signal characteristics. The most important innovation of this research is the finding that even after eliminating the propagation path effects between the various monitoring stations, significant differences in amplitude and frequency remain, suggesting that the dynamic parameters of the debris flow change during propagation. By combining seismic signals and image data, we were able to reconstruct the entire movement process of the debris flow and thoroughly investigate the changes in its characteristic parameters during movement. This finding not only deepens our understanding of the dynamic behavior of debris flows, but also provides important insights for the optimization of monitoring and early warning systems as well as for the design of protective measures.

C2: Additionally, I am skeptical about the reliability of the simple method used to calculate the "compensation function" for high-frequency signals (1-50 Hz). Although I am not an expert in seismic signal propagation modeling, using such simplistic input parameters and formulas for time-domain compensation seems problematic. Furthermore, I recommend the authors clarify whether they have removed the

instrumental response from the signals before deriving debris flow characteristics from absolute amplitude. The spectral plots suggest significant suppression at both high and low frequencies, which raises concerns about data processing.

R2: Thank you for your constructive comments. In this article, we primarily present a real-world case of a monitoring system that we developed based on practical conditions. It shows the results of our semi-quantitative and qualitative assessment of debris flow characteristics, such as flow velocity and particle properties. We used a linear viscoelastic compensation function for plane waves to compensate for the loss of high-frequency energy in seismic signals, thereby partially restoring the different degrees of attenuation of seismic waves at different frequencies during propagation, which improved the accuracy of the PSD analysis. Since this study involved observations near the source, we were able to capture more high-frequency information. Compared to data from seismic network stations that are further away from the debris flow and mainly reflect the absorption of low-frequency energy (since high-frequency energy associated with particle movement during propagation is absorbed), the high-frequency energy in our data is preserved to a greater extent. Low-frequency energy is relatively weaker in our data. Furthermore, high-frequency energy is related to the size, velocity, and concentration of debris flow particles, with energy typically limited to frequencies below 50 Hz, which may be due to the properties of the debris flow. The frequency characteristics of the three debris flows discussed in the paper also show differences.

In this study, we removed the instrument response and listed the relevant data in Table 1 and modified the relevant statements and figures.

Line 213

Table 1 Instrument parameters for observation stations in the two study catchments.

Equipment	Instrument parameters	
	Fotangba Gully	Er Gully
Seismograph	Sampling rate 100 Hz Corner frequency not offered Channel: Three components Sensor type: Capacitive force balance pendulum Dynamic range: Greater than 140 dB Bandwidth: 10 s - 50 Hz Sensitivity: 2000 V/(m/s)	—
Geophone	—	Sampling rate 100 Hz Corner frequency of 4.5–150 Hz Type: Delta-Sigma 24 Bit Channels: Three components Dynamic range: 125db @ 100sps

		(128db @ 50sps) Noise level: 10nV/sqrt (Hz) Input impedance: 100kOhm
Instrument response	Voltage sensitivity:2000V·S/m Normalized coefficient: 98696 Zero point: z1=0.0+0.0i z2=0.0+0.0i Main Pole: p1=-0.444221-0.6565i p2=-0.444221+0.6565i p3=-222.110595-222.17759i p4=-222.110595+222.17759i	Logger: "Cube3ext", Gain: 16 (DATA-CUBE³ User Manual)
Rain gauge	Record once per hour with a resolution of 0.2 mm	
Infrared camera	1 shot every 5 minutes at 2592×1944, 1920×1080 dpi resolution during the day and at night	

Lines 330 to 331

Based on the instrument response data in Table 1, the original seismic data was corrected for the instrument response and converted to velocity (m/s).

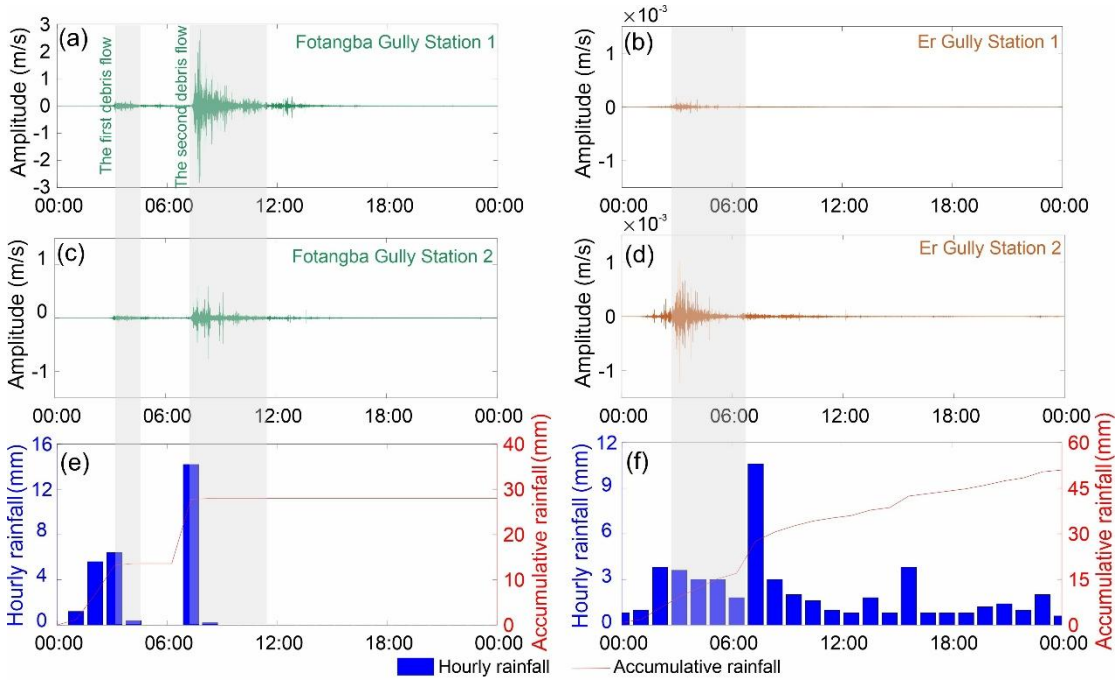

Fig. 4. Raw seismic signals and rainfall data. (a) and (c) represent monitoring station 1 and station 2 in the Fotangba Gully; (b) and (d) represent monitoring station 1 and station 2 in the Er Gully; (e) Rainfall at Fotangba Gully; (f) Rainfall at Er Gully.

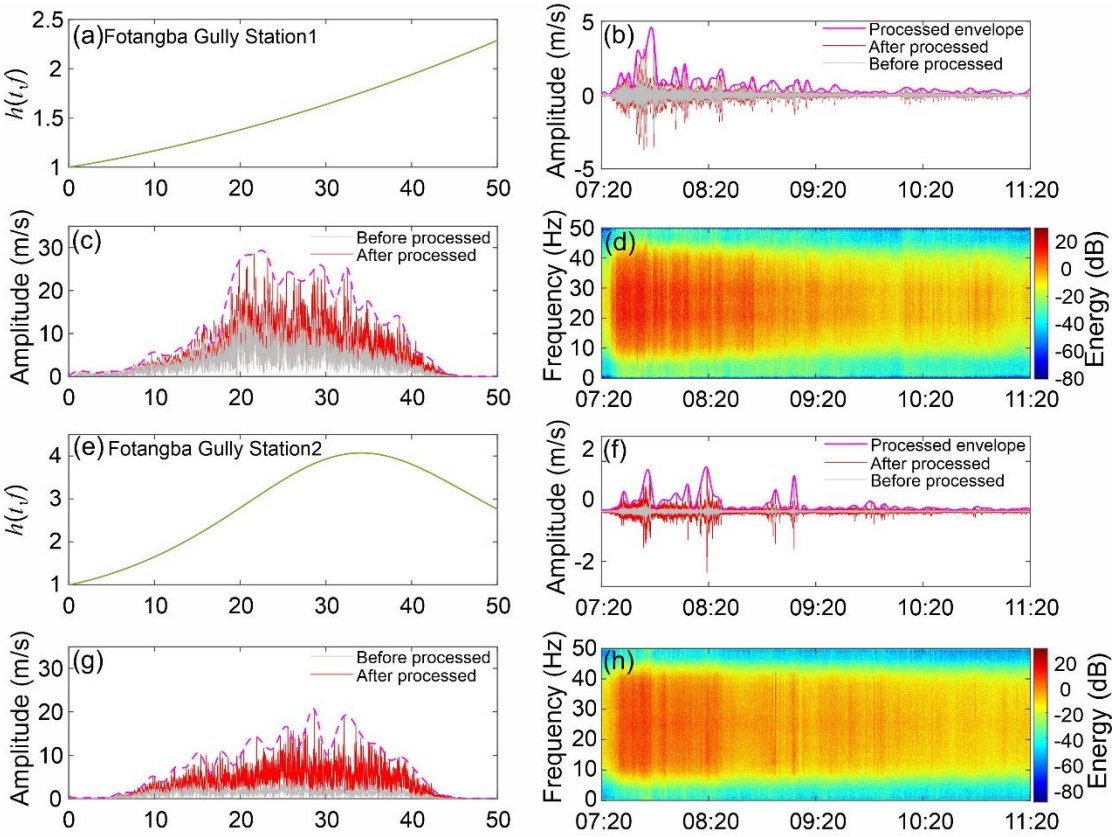

Fig. 5. Restored seismic signal for the second debris flow in Fotangba Gully. (a) Compensation function curve for monitoring station 1; (b) Time domain signal at monitoring station 1; (c) Frequency domain signal at monitoring station 1; (d) Restored spectrogram for monitoring station 1; (e) Compensation function curve for monitoring station 2; (f) Time domain signal at monitoring station 2; (g) Frequency domain signal at monitoring station 2; (h) Restored spectrogram for monitoring station 2. The red dashed lines in (c) and (g) are envelopes that represent peak amplitudes after processing.

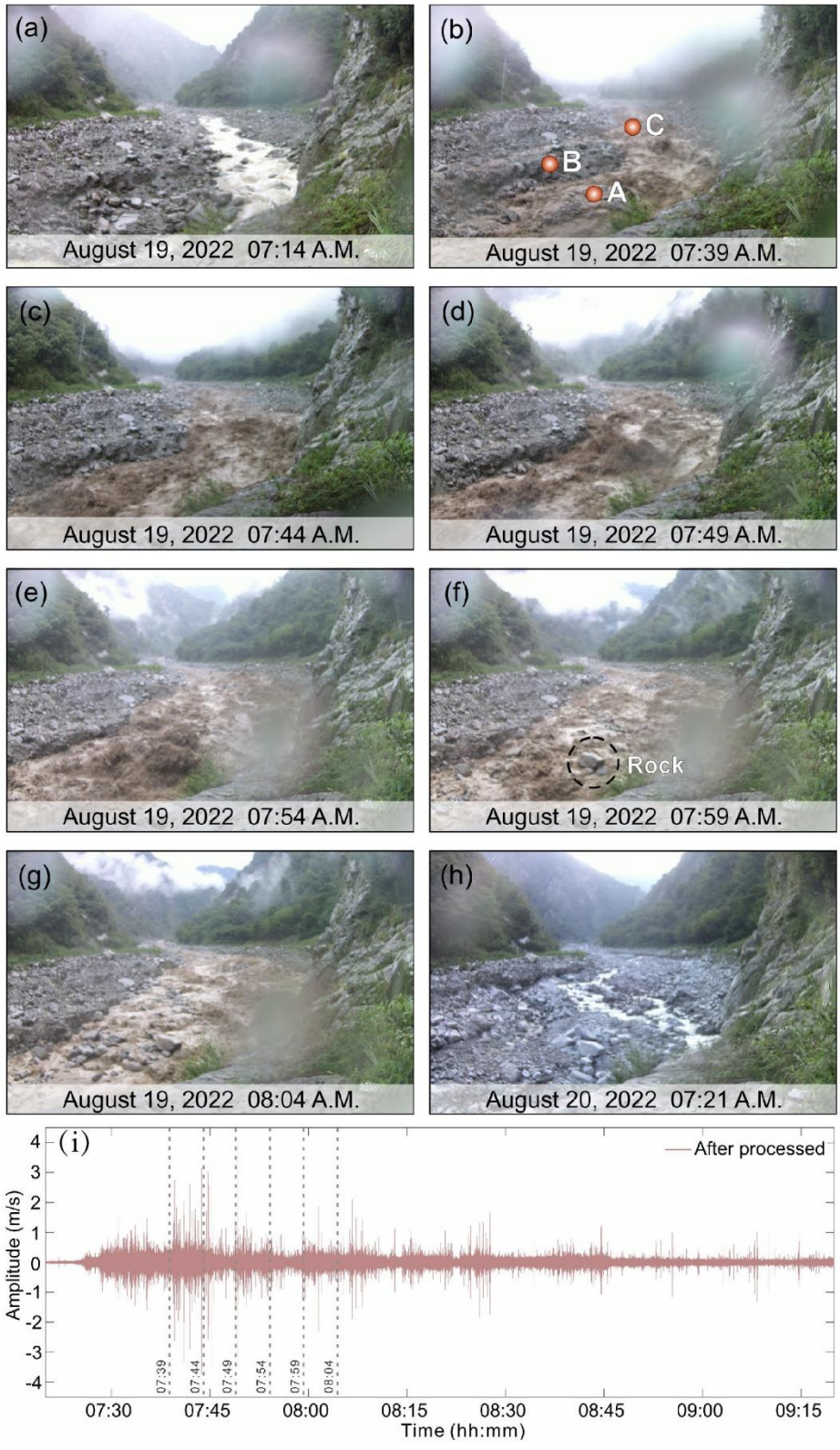

Fig. 7. Infrared camera images taken and the seismic signal recorded at monitoring station 1 in Fotangba Gully during the second debris flow on the morning of August 19, 2022. Images were recorded every 5 minutes: (a) 7:14 frame (b) 7:39 frame; (c) 7:44 frame; (d) 7:49 frame; (e) 7:54 frame; (f) 7:59 frame; (g) 8:04 frame; (h) August 20, 2022, 8:04 Frame; (i) seismic signal recorded at the point.

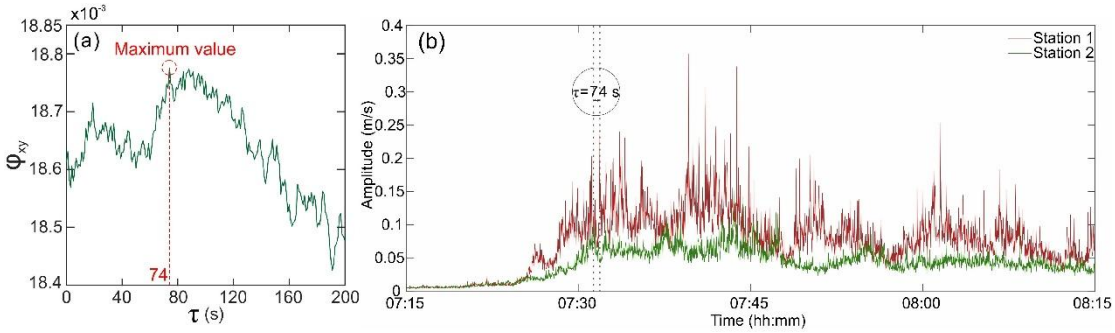

Fig. 8. The cross-correlation algorithm calculates the second debris flow in Fotangba Gully. (a) signal lag time τ between two observation stations; (b) Amplitude range of debris flow (vertical direction).

Specific comments:

C1: Title: This manuscript does not accurately reflect real-time seismic signal analysis, as the signals were not transmitted or processed in real time. Consider revising it accordingly.

R1: Thank you very much for your suggestions. We have revised the focus of our study, which now concentrates primarily on reconstructing the debris flow process. We have therefore changed the title to "Reconstruction of the Wenchuan debris flow process in August 2022 through in-situ monitoring and analysis of seismic signals."

C2: Abstract: If this manuscript is a case study, the abstract should emphasize specific case details.

R2: Thank you for your helpful comments. We have revised the focus of our study, which now concentrates primarily on reconstructing the debris flow process. We have therefore changed the title to "Reconstruction of the Wenchuan debris flow process in August 2022 through in-situ monitoring and analysis of seismic signals." And our abstract is modified as follows:

Lines 15 to 29

Abstract

Rainfall-induced debris flows are highly destructive due to their abrupt onset, rapid movement, and high sediment transport capacity, all of which can lead to significant loss of life and damage to infrastructure. However, a comprehensive analysis of their dynamic evolution remains limited by the scarcity of in-situ monitoring data. In this study, we utilized near-field seismic data recorded by acquisition instruments

deployed in Wenchuan, China, combined with images and post-event field investigations to reconstruct the second debris flow event in Fotangba Gully. Seismic signal attenuation was compensated, and time-frequency analysis and power spectral density (PSD) calculations were conducted. The results reveal pronounced differences in signal amplitude and frequency content across stations, reflecting spatial heterogeneity in flow dynamics. We identified flow velocity and grain concentration as the dominant factors affecting the PSD curves. This research provides a framework for extracting debris flow kinematics characteristics from seismic signals and offers new insights for hazard evaluation and the design of mitigation strategies.

C3: L44: Similarly, this study does not involve real-time seismic signal analysis.

R3: Thank you for your helpful comments. We have shifted the highlights of our study from monitoring and early warning to reconstructing the debris flow process and analyzing its characteristics. The relevant content has been revised accordingly, as explained in more detail below:

Lines 32 to 43

Highlights:

- By analyzing the characteristics of seismic signals, the study successfully reconstructed the entire process of the second debris flow event at Futangba Gully by utilizing features such as the time series, flow velocity, particle characteristics, and surge variations of the debris flow.
- The seismic signal characteristics of the debris flow showed rapid excitation and slow attenuation. Even after removing propagation effects, significant differences in amplitude and frequency were observed at different monitoring stations, indicating changes in the dynamic parameters of the debris flow.
- The time-frequency characteristics of seismic signals reflect the evolution process of debris flows, with a corresponding relationship between the power spectral density and debris flow characteristics.

C4: L65: The connection between this sentence and debris flow monitoring/early warning is unclear. It appears abrupt.

R4: Thank you for your constructive suggestions sincerely. Due to the change in the focus of research, this section has been deleted.

C5: L66-67: Clarify whether "these systems" refer to debris flow early warning systems? Real-time rainfall monitoring is not a technical challenge, so the statement

seems vague.

R5: Thank you for your comments. Due to the change in the focus of research, this section has been deleted.

C6: L75-78: Reassess the logic of this sentence, as there is no clear cause-and-effect relationship.

R6: Thank you for your comments. Referring to **R5**, we have deleted this sentence.

C7: L79-87: The logic of this paragraph is unclear. It is difficult to discern the authors' intended message.

R7: Thank you for your suggestions. We have made revisions to this section, as detailed below:

Lines 87 to 101

Existing monitoring methods mainly involve installing instruments in debris flow channels to monitor hydrological parameters, such as water flow and water level, a variety of instruments, including infrasound sensors (Marchetti et al., 2019), LiDAR (Aaron et al., 2023), fiber optic sensors (Huang et al., 2012; Schenato and Pasuto, 2021), pressure sensors (Berti et al., 2000; Kean et al., 2012), and stress sensors (McArdell et al., 2007; McCoy et al., 2010; Nagl and Hübl, 2017), are increasingly utilized to capture a wide array of parameters. However, existing monitoring methods face challenges when it comes to collecting comprehensive data throughout the entire debris flow process. They require accurate identification of debris flows and the prior installation of monitoring instruments, as well as ensuring that these instruments remain intact during the debris flow. The sudden occurrence and violent impact of debris flows can damage nearby monitoring equipment and make data collection difficult. In addition, some existing methods for monitoring debris flows are limited to collecting data from a specific cross-section rather than providing continuous data for the entire debris flow process.

C8: L122-129: The authors discuss seismic instrument installation and related challenges to highlight limitations of debris flow monitoring. While these are valid points, they seem irrelevant to the main topic. Since the manuscript does not address these issues further, the introduction lacks clear motivation.

R8: Thank you for your comments. Based on the expert's suggestions, the focus of this study has shifted from monitoring and early warning to reconstructing the debris flow process and analyzing its characteristics. As a result, the section discussing the difficulties in installing the instruments has been removed.

C9: L148-149: Add relevant references for this statement.

R9: Thank you for your comments. We add relevant references for this statement.

Lines 172 to 174

The area experiences frequent seismic activity, and signs of the May 12, 2008 Wenchuan Earthquake are still evident, with loose rocks and soils providing abundant sediment for debris flows (Zhang et al., 2023).

C10: L150-152: What is the debris flow frequency in the study area?

R10: Thank you for your comments. Debris flow yearly frequency ranges from 0.17 to 2.67. As follows:

Lines 175 to 178

This study focuses on the Er and Fotangba Gullies in the Minjiang River Basin, which has experienced numerous debris flow events in recent years, yearly frequency ranges from 0.17 to 2.67, threatening nearby villages, roads, and hydropower stations (Guo et al. (2016).

C11: Table 1: Missing key parameters of seismic instruments, such as corner frequency. Are the instruments three-component? Were instrumental responses processed in the analysis? Are these signals transmitted in real time, and can the deployment sites connect to a wireless network?

R11: Thanks a lot for the constructive comment. Thank you for your feedback. We have added the relevant instrument parameters in Table 1. Since angular frequency is related to frequency ($w = 2\pi f$), we have only listed the frequency parameter. Due to the lack of network signal in the debris flow channels, our data cannot be transmitted in real-time. Instead, it is stored by on-site equipment and retrieved after the debris flow event. The response to the instrument response has been removed as shown in **General comments R2**. Signal transmission related expression is as follows:

Lines 204 to 205

However, due to the lack of a network signal, real-time transmission of the recorded data via the Internet/GSM is not possible.

C12: L233-237: How did the authors remove instrumental effects? Without removing the instrumental response, analyzing absolute signal amplitude is meaningless.

R12: Thank you for your helpful comments. We have added relevant expressions about instrumental response. Refer to more details in **General comments R2**.

C13: L249-281: The introduction of STFT, cross-correlation, and PSD is overly detailed, given that these are basic signal processing methods. Consider summarizing this section and citing relevant specialized literature instead.

R13: We totally agree with the reviewer's suggestion. We have revised the relevant sections of the manuscript according to the reviewer's suggestions, omitting more established algorithms and placing greater emphasis on the application of the relevant methods in this study.

Lines 242 to 270

Tsai et al. (2012) developed a PSD model for sediment transport that links seismic signals with water turbulence, precipitation, and sediment transport in rivers. In their model, they considered the relationship between seismic signals and the transport of bedload in rivers. Tsai et al. (2012) adapted this model for debris flows by including absorption damping during the propagation process and established the PSD model for debris flows near the source shown in Eq. (1). This model links debris flow parameters such as length, particle size, width, velocity, and attenuation factors (due to absorption) as well as viscoelastic parameters during propagation with the seismic PSD of the debris flow.

$$PSD \approx 1.9 \cdot LWD^3u^3 \cdot \frac{f^{3+5\xi}}{v_c^5 r_0} e^{-\frac{8.8 f^{1+\xi} r_0}{v_c Q}}, \qquad (1)$$

where W is width of the channel, D represents the 94th centile of the grain size distribution, u represents debris flow velocity, f is frequency, v_c is Rayleigh wave phase velocity at 1 Hz, r_0 is distance between the monitoring station and channel, L is effective length of $L=r_0$, $\xi=0.4$ is a parameter related to how strongly seismic velocities increase with depth at the site, and Q is an attenuation factor (Tsai et al., 2012; Lai et al., 2018).

Debris flow seismic Power spectral density calculated by Eq. (2), which means

the power per frequency for different frequencies in a specific period (Yan et al., 2020), and allows debris flow evolution to be analyzed from the seismic signal. The power of full band seismic is calculated by the short-time Fourier transform (STFT, Eq. 3), allowing getting the frequency domain characteristics of the signal versus time, which can help us to get the PSD changes versus the time.

$$PSD_{f_{\min}\sim f_{\max}}(t)=\frac{1}{(f_{\max}-f_{\min})}\times\sum_{f=f_{\min}}^{f_{\max}}X(t,f), \quad (2)$$

$$X(t,f)=\sum_{-\infty}^{\infty}x(m)W(t-m)e^{-j2\pi fm} \quad (3)$$

where f is the angular frequency, $f_{\min}$ and $f_{\max}$ represent minimum frequency and maximum frequency, respectively, t is time for the seismic signal, $X(t, f)$ represents the spectrogram based on STFT (Yan et al., 2017)., x are time domain signals, W is the window function, m is the start time of the window function, e is a natural constant, t is time, and j is the imaginary number (Yan et al., 2021). A Hanning window length of 2056 and a time length of 20.56 s correspondingly is used. A built-in function "spectrogram" of MATLAB is used to achieve STFT directly from the software manual. The sampling rate is 100 Hz, so we choose 1 Hz and 50 Hz (i.e., a half of 100 Hz) as $f_{\min}$ and $f_{\max}$.

Lines 308 to 316

Arattano and Marchi (2005) found that the velocity values calculated using cross-correlation were close to the measured velocity values. In the context of debris flows, the average flow velocity between monitoring stations can be obtained by dividing the distance between the stations by the signal time delay. This method has been used to objectively calculate the mean velocity of debris flows (Coviello et al., 2015):

$$[x_K]=[x_0,x_1,x_2,\ldots,x_{M-1}] \quad (6)$$

$$[y_K]=[y_0,y_1,y_2,\ldots,y_{M-1}] \quad (7)$$

$$\phi_{yx}(\tau)=\sum_{t=0}^{M-1}x_t y_{t+\tau}\ , \quad (8)$$

where y from station 2 is another signal of time domain for the same event as x from station 1, t and K which are absolute sampling time series from 0 to M-1, ϕ represent cross-correlation function. When t exceeds M-τ-1 and is less than 0, x_t and $y_{t+\tau}$ is equal to 0.

C14: L283-284: Revise this sentence to discuss existing studies that use PSD to evaluate debris flow dynamics.

R14: Thank you very much for your suggestions. Based on your suggestions, we have made the following changes:

Lines 242 to 250

Tsai et al. (2012) developed a PSD model for sediment transport that links seismic signals with water turbulence, precipitation, and sediment transport in rivers. In their model, they considered the relationship between seismic signals and the transport of bedload in rivers. Tsai et al. (2012) adapted this model for debris flows by including absorption damping during the propagation process and established the PSD model for debris flows near the source shown in Eq. (1). This model links debris flow parameters such as length, particle size, width, velocity, and attenuation factors (due to absorption) as well as viscoelastic parameters during propagation with the seismic PSD of the debris flow.

C15: Formulas 6 and 7: Equation 6 appears to account for signal attenuation. If so, why is Equation 7 necessary? Clarify whether there is overlap or redundancy between these two equations.

R15: Thanks a lot for the constructive comment. Indeed, Equation 7 (Eq. 4) takes into account the attenuation of seismic waves by the Earth, which forms the basis of our explanation for the PSD curve. In contrast, Equation 6 (Eq. 1) does not account for signal attenuation. Equation 6 (Eq. 1) calculates the frequency curve's integral with respect to frequency, divided by the frequency bandwidth, which is similar to computing the geometric mean of the frequency. It does not compensate for signal attenuation in seismic data. It is precisely because of this difference that we propose using Equation 7 (Eq. 4) for signal attenuation compensation. This compensation equation is based on the 1D plane wave compensation equation of the constant Q viscoelastic model by Kjartansson (1979).

C16: Formula 8: Clarify the derivation process and include references. Why is σ=0.02?

Provide a basis or justification for this value.

R16: Thank you for the constructive advice. This is a method for controlling high-frequency compensation, which was first proposed by Wang (2006). It was developed to address the high-frequency instability in 1D plane wave Q compensation and has been widely applied in post-stack Q compensation in seismic exploration for oil. In this context, σ is a constant known as the stability control factor, and its value needs to be determined based on the signal-to-noise ratio characteristics of the signal.

Reference

Wang, Y. (2006). Inverse Q -filter for seismic resolution enhancement. GEOPHYSICS, 71(3), V51–V60

C17: L303-304: Explain why Formula 8 performs better for high-frequency signals. What underlying principles support this?

R17: We thank the reviewer for this helpful comment. We have added relevant content to the manuscript to explain why Formula 8 (Eq. 5) performs better and provided corresponding references.

Lines 291 to 300

Direct use of Eq. (4) to compensate for absorption attenuation results in significant attenuation in the high-frequency range, leading to a lower signal-to-noise ratio (SNR) and an excessively large amplitude compensation factor. This can cause the compensated amplitude to become too large and the SNR to be extremely low (Wang, 2002). In this study, I will use the gain control method proposed by Wang (2002) (Eq. 5) to maintain the stability of the high-frequency range. This method aims to improve the energy of the high-frequency range while keeping the overall SNR of the entire frequency band relatively controlled.

$$\Gamma(t,f)=\frac{h(t,f)+\sigma^2}{h^2(t,f)+\sigma^2}, \qquad (5)$$

where σ is a constant named stability control factor, whose value comes from a numerical experiment., with a σ^2 value of 0.02 used here.

Reference

Wang, Y., 2002. A stable and efficient approach of inverse Q filtering. Geophysics, 67(2), 657-663.

C18: L312: Specify the preprocessing steps—do they involve removing instrument response, filtering, or other methods?

R18: Thank you for spending the time to review and assess our manuscript. We have removed instrument response, as shown in **General comments R2**.

C19: L320-322: How do the authors address the influence of variations in debris flow characteristics on seismic signals?

R19: Thank you so much for the comments. The particle size, movement velocity, concentration of the debris flow, and the distance between the debris flow and the monitoring station all affect the seismic signals. Qualitatively, the larger the particles, the higher the particle velocity, the greater the concentration, and the closer the distance to the monitoring station, the stronger the seismic signal energy and the more high-frequency information it contains. As follow:

Lines 709 to 735

In our study, the seismic signals generated by the vibrations of debris flow particles with the riverbed within a certain range around the sensors are superimposed and received. We assumed that the variation of vc and Q near the channel mainly composed of debris flow deposition changes slightly. The seismic signals, generated by debris flow channel farther away from the sensor, travel much longer leading the seismic mainly dominated by low-frequency signals and with relatively low peak frequencies; whereas the seismic signal from the nearby channel is opposite, dominated by high-frequency signals and with relatively high peak frequencies. Flow velocity, flow volume, and particle content vary throughout the entire river channel. The seismic signals received from the debris flow with a high velocity, massive volume, and rich particle content primarily consist of low frequencies with lower peak frequencies. Conversely, the signals are mainly high frequencies under the opposite conditions. The low- and high-frequency energy shows a substantial enhancement from 7:44 to 7:49, along with an alteration in the peak frequency toward a higher frequency, indicating an increasing signal strength at different propagation distances. In contrast, low-frequency energy decreases and high-frequency energy stays stable at 7:54, suggesting that the seismic energy from distant sources weakens and from

nearby sources remains steady. The variation of grain concentration (flow volume and particle content) near the channel affects the shape of PSD. An anomaly observed at 7:44 in low-frequency energy is due to the upstream flow volume rising. As debris flow with high grain concentration moves toward the sensors and flows downstream, the low-frequency energy decreases and eventually recovers to a normal level.

We believed that the flow velocity decreases and grain concentration follows a trend of increasing first and then dropping during the six key moments with a 5-minute sampling interval from 7:39 to 8:04. The results are consistent with the findings from infrared image analysis in Section 4.3.2, demonstrating that analyzing the evolution of the debris flow using the time-frequency characteristics of seismic signals is feasible.

C20: L322-325: Elaborate on the input parameters used to calculate the signal-to-noise ratio (SNR).

R20: We thank the reviewer for this comment. We selected the seismic signals from the same time period on the day prior to the debris flow event as the background noise, and calculated the ratio of the debris flow signal power to the noise power as the signal-to-noise ratio (SNR). As follow:

Lines 354 to 361

We selected the seismic signals from the same time period on the day prior to the debris flow event as the background noise, and calculated the ratio of the debris flow signal power to the noise power as the signal-to-noise ratio (SNR) (Fu et al., 2020). In terms of signal-to-noise ratio (SNR), the SNR for the first debris flow in Fotangba Gully was 20.66 dB and 7.96 dB, while for the second debris flow it was 19.60 dB and 15.80 dB. Similarly, at measuring station 2 in Er Gully, the amplitude and fluctuations of the seismic signals were higher than at station 1, with SNR values of 20.47 dB and 17.62 dB, respectively.

C21: L336: Does "maximum rainfall" refer only to the day of the debris flow event? If similar maximum or cumulative rainfall occurred on other days, did debris flows also occur? Clarify.

R21: Thanks a lot for the constructive comment. Here, the "maximum rainfall" refers to the maximum hourly rainfall on the day of the debris flow event. During the monitoring period of this study, no other day recorded similar maximum or cumulative rainfall. Only these two debris flow events in Fotangba Gully occurred during the monitoring period.

C22: L349-395: The use of Formulas 7 and 8 to account for signal attenuation raises concerns. Although I am not an expert in seismic wave propagation modeling, the reliance on simplified epicentral distances and attenuation coefficients for high frequency signals (1-50 Hz) seems questionable. Compensating for attenuation using these simplified formulas, especially with generalized seismic ground velocity model, undermines confidence in the results.

If the authors had used these parameters to derive the PSD of the raw signal, the approach might be more acceptable. Furthermore, clarify the motivation for recovering the absolute amplitude of the original signal! Does the analysis explicitly require it? This rationale is unclear in the manuscript.

R22: Thank you for your helpful comments. The PSD curve calculated using Eq. (2) serves as the basis for our semi-quantitative analysis of the characteristic parameters of debris flows, which is primarily carried out using Eq. (1). The equation established by Tsai (2012) is based on the idea that the PSD of the seismic signals generated by the debris flow is the result of the attenuation of individual seismic signals generated by each particle and then superimposed. As suggested by the reviewer, the derivation of Equation 1 fully takes into account parameters such as the epicentral distance and the attenuation coefficient.

When calculating the PSD using Eq. (2), we did not remove the effects of layer absorption attenuation, which means that the PSD curve calculated directly from Eq. (2) actually includes the propagation effects. If we were to remove the propagation effects and then use Eq. (2) to obtain the PSD curve, it would primarily reflect the influence of debris flow properties on the seismic signal. Our goal is to restore the original signal as much as possible in order to minimize the influence of propagation on the seismic frequency characteristics.

C23: Figure 5: The seismic instrument appears to suppress signals below 4.5 Hz and above 45 Hz. However, debris flow fronts often exhibit strong signals in the 1-5 Hz range. Reassess whether the instrument response was removed prior to analyzing absolute amplitude.

R23: Thank you for the constructive comments. We have modified the information about the instrument response. Refer to more details in **General comments R2**. The statement “debris flows often exhibit strong signals in the 1–5 Hz range” primarily

refers to the seismic response caused by changes in debris flow velocity. Our near-source observations are capable of recording the impact of debris flow particles on the riverbed, which mainly generates high-frequency signals. These high-frequency signals are often attenuated during propagation, so we cannot observe them from locations far away from the source of the debris flow. At these distant locations, we can only observe the low-frequency signals caused by changes in the speed of the debris flow.

C24: L449-451: How do the authors account for waveform propagation path effects? Using simplified Formulas 7 and 8 to compensate for signal attenuation does not adequately address significant path effects.

R24: Indeed, path effects are a complex issue that cannot be completely eliminated with a simple compensation function. Since this study uses near-field monitoring, with the monitoring stations located relatively close to the channel center (approximately 10-20 meters), the low-frequency signals experience less attenuation. We have explored the use of Formulas 7 (Eq. 4) and 8 (Eq. 5) to compensate for some of the high-frequency signals as much as possible. Additionally, since this study only involves a simple comparison of the raw signals from two stations within the same channel, the signal compensation primarily focuses on analyzing the characteristics of the single-station signals. The compensated signal parameters are consistent. Therefore, analyzing the characteristics of the compensated single-station signals remains reliable.

C25: L467-470: This contradicts earlier claims. If the authors find Formulas 7 and 8 effective for attenuation compensation, why attribute signal differences to path effects here? Clarify this inconsistency.

R25: Thanks a lot for the constructive comment. The compensation function cannot completely restore the signal, and thus, we have not fully eliminated the path effect. For more details, please refer to Reply 24(**R24**). We have made adjustments and modifications to this section. The primary focus of this study is to analyze the development process of the debris flow at a single monitoring station over different time periods, while comparisons between different stations are mainly used to analyze the occurrence time of the debris flow.

C26: L508: A debris flow velocity of 38.3 m/s is unusually high. Verify this value against typical debris flow velocities to ensure accuracy.

R26: Thank you for the useful advice. Indeed, we found that the velocity of the debris flow in Er Gou, calculated using the cross-correlation algorithm, reached 38.3 m/s, which is significantly higher than the velocity of 1–6 m/s observed by Cui et al. (2018)

in section S1 of Er Gully. This suggests that the results obtained using cross-correlation for Er Gully may be inaccurate. In the "Discussion" section, we analyze that the possible reason for this discrepancy could be the relatively curved river course between the two measurement points in Er Gully.

Lines 756 to 771

The average velocity of the second debris flow event at Fotangba Gully, calculated using the cross-correlation function, was validated as reliable by the Manning formula. However, using the same method, the flow velocity of the Er Gully debris flow was calculated to be 38.3 m/s. Due to the damage observed in the Er Gully debris flow images and at the site, we were unable to verify this result using the Manning formula. Since this velocity exceeds the 1-6 m/s range found by Cui et al. (2018) for the Er Gully debris flow, we infer that the flow velocity derived from the cross-correlation calculation for this event is likely incorrect. Upon reviewing previous studies that used the cross-correlation algorithm to calculate debris flow velocities, we found that the channels between the two measurement stations in these studies were relatively straight (with small curvature) (Arattano et al., 2012; Comiti et al., 2014; Schimmel et al., 2022). By comparing the locations of the Er Gully and Fotangba Gully observation points, we hypothesized that the significant curvature of the channel between the two observation points in Er Gully may be a key factor. Therefore, directly using the cross-correlation algorithm to calculate the flow velocity for debris flows in highly curved channels between monitoring stations may not be reliable.

C27: L518-527: The authors use Manning's formula to validate velocity estimates from signal cross-correlation. However, why was this approach not applied to verify the unexpected velocity of 38.3 m/s? Failing to address such anomalies weakens the reliability of the cross-correlation results.

R27: We thank the reviewer for this helpful comment. Due to the destruction at the site after the debris flow in Er Gully, field investigations were fraught with considerable challenges, and the time-lapse camera was unable to capture real-time images of the debris flow due to water droplets obscuring the lens. As a result, we were unable to determine the parameters required for the calculation using Manning's equation. For this reason, we referred to previous studies to explain that the results of

the cross-correlation calculation for Er Gully may not be accurate. For further details, please refer to answer **R26**.

C28: L679-680: Why not compare the simulated PSD for the event (with the estimated velocity of 38.3 m/s) against the measured PSD? A large discrepancy would cast doubt on the validity of the results.

R28: Thank you for spending the time to review and assess our manuscript. We sincerely apologize for the limitations regarding the data obtained for the Er Gou debris flow (due to a lack of field investigations and real-time images), which prevented us from conducting a more detailed analysis of the Er Gou debris flow. Therefore, this study focuses primarily on the second debris flow event in Fotangba, where we analyze its signal characteristics and reconstruct the process.

C29: Figure 12: The measured and simulated PSD amplitudes show significant differences (compare Figures 12a and 12b). Address these discrepancies and their implications for the analysis.

R29: Thank you for your useful advice. We have replaced Figure 12b (Fig. 10b) with the new one to explain the mechanism of the curve shape change in Figure 12a (Fig. 10a).

Lines 693 to 730

Propagation distance (r_0), Rayleigh wave phase velocity at 1HZ (v_c), and attenuation factor (Q) determine the spectrum shape characteristics of PSD (Eq. 1). We investigated the effect of these three parameters and linked the frequency features variation and dynamic parameters of debris flow via a simple forward algorithm based on Eq. 1. The key parameters were derived from the second debris flow at Fotangba Gully: the D94 value is determined by the 94th centile of the grain size distribution; the flow velocity of 6 m/s is obtained through cross-correlation calculation; the r0, vc, and Q are set near the values during the seismic signal restoration. The results are shown in Fig. 10b. The peak frequency of PSD shifts towards a higher frequency and a broader band as r0 decreases or a contrary alteration of vc and Q.

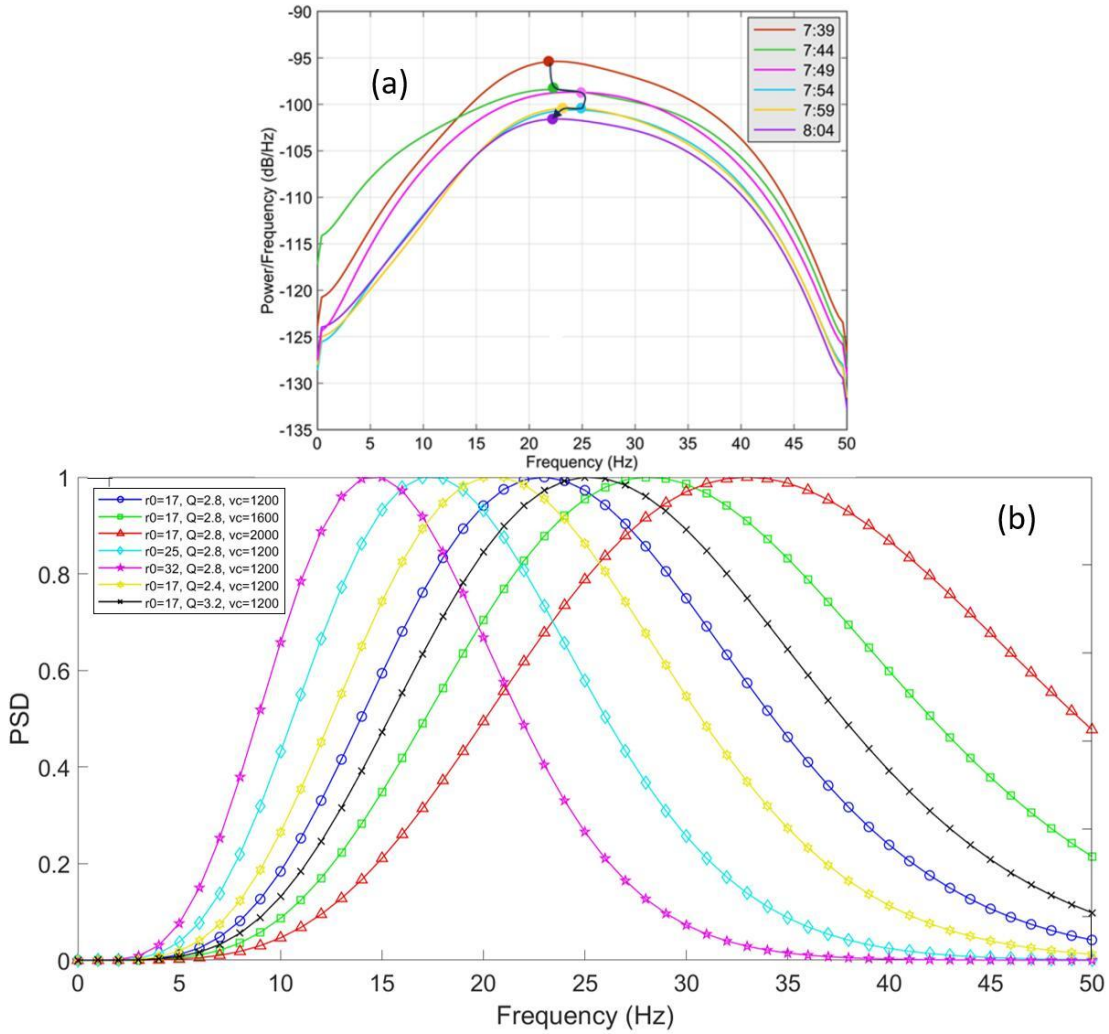

Fig. 10. Characteristic change of power spectral density (PSD). (a) Evolution of PSD during the second debris flow in Fotangba Gully on the morning of August 19, 2022, from 7:39 to 8:04; (b) Comparison of PSD for different r0, Q, and vc. The six dots in subplot (a) correspond to the PSD maximum at the six-time points from 7:39 to 8:04, and the black arrows indicate the time course of these six-time points.

In our study, the seismic signals generated by the vibrations of debris flow particles with the riverbed within a certain range around the sensors are superimposed and received. We assumed that the variation of vc and Q near the channel mainly composed of debris flow deposition changes slightly. The seismic signals, generated by debris flow channel farther away from the sensor, travel much longer leading the seismic mainly dominated by low-frequency signals and with relatively low peak frequencies; whereas the seismic signal from the nearby channel is opposite, dominated by high-frequency signals and with relatively high peak frequencies. Flow velocity, flow volume, and particle content vary throughout the entire river channel. The seismic signals received from the debris flow with a high velocity, massive

volume, and rich particle content primarily consist of low frequencies with lower peak frequencies. Conversely, the signals are mainly high frequencies under the opposite conditions. The low- and high-frequency energy shows a substantial enhancement from 7:44 to 7:49, along with an alteration in the peak frequency toward a higher frequency, indicating an increasing signal strength at different propagation distances. In contrast, low-frequency energy decreases and high-frequency energy stays stable at 7:54, suggesting that the seismic energy from distant sources weakens and from nearby sources remains steady. The variation of grain concentration (flow volume and particle content) near the channel affects the shape of PSD. An anomaly observed at 7:44 in low-frequency energy is due to the upstream flow volume rising. As debris flow with high grain concentration moves toward the sensors and flows downstream, the low-frequency energy decreases and eventually recovers to a normal level.